Production of polarized $^3He^{2+}$ ion by ECR-ionizer

M. Tanaka

Kobe Tokiwa College, Ohtani-cho 2-6-2, Nagata-ku, Kobe 653-0838, Japan

N. Shimakura

Department of Chemistry, Niigata University, Ikarashi Nino-cho 8050, Niigata 950-2181, Japan

Yu. A. Plis

Joint Institute for Nuclear Research, Dubna, RU-141980, Moscow region, Russia

Abstract

The possibility of using an ECR (Electron Cyclotron Resonance) ionizer of polarized ^3He gas as a compact polarized ^3He ion source is investigated by the Monte Carlo simulation over an ECR frequency range from 2.45 to 16 GHz. In this calculation, we assume that the depolarization mechanism is caused by multiple ionization, inelastic scattering, and de-ionization processes of the ^3He atoms and ions confined in the ECR plasma under the presence of the external magnetic field and the microwave for ECR. To check the validity of the present Monte Carlo simulation, we calculate the proton polarization following the ionization of polarized hydrogen gas by the ECR ionizer and find consistency between the calculated results and experimental ones.

With a typical value of the ^3He gas polarization currently available, i.e., $P_{gas} \sim 0.5$, a polarized $^3He^{2+}$ beam with the maximum polarization less than 0.2 can be expected from the polarized ^3He ion source based on the ECR-ionizer.

1 Introduction

Since the first success of polarized ^{3}He ion sources based on the optical pumping method over 30 years ago[1], a variety of types of polarized ^{3}He ion sources have been proposed and developed. However, most of them have not survived because of insufficient beam current, polarization and reliability. An exceptional case is the polarized ^{3}He ion sources developed at RCNP, Osaka University. This polarized ^{3}He ion source is based upon the electron pumping or spin exchange methods aiming at large polarization (≥ 0.7) of the $^3He^{2+}$ ions and is even now under development[2]. However, one of the disadvantages associated with the RCNP ion sources is that the produced ion is $^3He^+$. In other words, further ionization of the $^3He^+$ ion is necessary to convert it to $^3He^{2+}$ before injecting it into accelerators like cyclotrons. Unfortunately, such ionization of the $^3He^+$ ion is not easy without the loss of polarization and beam intensity. As an alternative method to produce polarized $^3He^{2+}$ ions with high intensity, a compact polarized ^{3}He ion source based on ionization of polarized ^{3}He gas with an ECR-ionizer was recently proposed. As a matter of fact, this proposal is based on the latest success in ionizing a polarized hydrogen gas by the ECR ionizer operated at relatively low ECR frequencies [3,4]. Ionization of the polarized ^{3}He gas to generate the polarized $^3He^{2+}$ ion by the ECR-ionizer seems to be more promising and advantageous than the RCNP polarized ^{3}He ion sources from the view point of compactness.

However, in spite of the advantages mentioned above there has been no examination of the feasibility of the ECR-ionizer applied to ionization of polarized gases heavier than hydrogen or deuterium. Basically, the major depolarization can be induced by the hyperfine interaction between a nucleus and an unpaired electron of atom and ion. In this respect, candidates which give rise to the depolarization are, respectively, a hydrogen atom and a $^3He^+$ ion for ionization of the polarized hydrogen gas and polarized ^{3}He gas. However, a fundamental difference exists between ionization of the ^{3}He and the hydrogen atom as summarized by

(1) the hyperfine interactions and fine structure interactions of the $^3He^+$ ion are larger by 6 and 16 times, respectively, than those of the hydrogen atom,
(2) the $^3He^+$ ions are confined in the ECR plasma for a long period, while the hydrogen atom is not confined in the ECR plasma because of neutrality,
(3) the ionization and de-ionization processes are much complicated for the ^{3}He than those of the hydrogen.

These aspects may give rise to significantly greater depolarization of $^3He^{2+}$ ions than that for the hydrogen atom.

The aim of the present work is to theoretically investigate the mechanism governing the $^3He^{2+}$ polarization, in particular the depolarization mechanism of the $^3He^+$ ion confined in the ECR plasma. For this purpose, we employ a Monte Carlo simulation in which the multiple ionization, inelastic scattering and de-ionization processes for the ^3He , $^3He^+$, and $^3He^{2+}$ ions occurring in the ECR plasma are correctly taken into account. To check validity of the Monte Carlo simulation, the calculation is applied to the hydrogen ECR-ionizer whose characteristic behavior has been well established experimentally and theoretically.

2 General view of depolarization in ECR plasma

2.1 Ion-atom collisions in ECR plasma

An ECR-ionizer is known as a powerful tool to generate highly stripped heavy ions step-by-step with the high temperature electrons in the ECR plasma heated by the ECR resonance microwaves[5,6]. To enable the confinement of plasma consisting of electrons + ions for a long period, a magnetic mirror field axially and multipole field radially are applied. In case of ionization of the ^3He gas, an initial ^3He atom is sequentially ionized by the electrons as given by

$$^3He + e^- \longrightarrow ^3He^+ + e^- + e^-, \tag{1}$$

$$^3He^+ + e^- \longrightarrow ^3He^{2+} + e^- + e^-. \tag{2}$$

However, if the ion confinement time is long enough, the following de-ionization (electron recombination) processes may become significant by the interaction of ions with a residual gas existing the ECR plasma region;

$$^3He^{2+} + RG \longrightarrow ^3He^+ + RG^+, \tag{3}$$

$$^3He^+ + RG \longrightarrow ^3He + RG^+, \tag{4}$$

where a notation, "RG" represents the residual gas atoms including ^3He gas itself.

2.2 Depolarization due to insufficient magnetic decoupling field

Next, we discuss possible depolarizations due to insufficient magnetic decoupling field. When an atom or ion has an unpaired electron like a hydrogen and $^3He^+$ ion, the depolarization can be induced by the hyperfine interactions between the unpaired electron and nucleus. However, if an external magnetic field, B is much larger than a critical field, B_c proportional to the hyperfine interaction strength, the depolarization is reduced as a result of the decoupling of the nuclear spin from the electron spin. As discussed in Appendix A, the $^3He^+$ nuclear polarization under the external field, B is obtained,

$$P_{01} = 1 - \frac{1}{2(1+x^2)}, \tag{5}$$

where x=B/B_c with B_c = -309.6 mT, and +50.7 mT for $^3He^+$ ion and hydrogen, respectively.

We start with introduction of a fully nuclear polarized (P_0=1.0) ^3He atom in the $^1S_1$ state into an ECR-ionizer. In this stage no depolarization occurs because the ^3He atom has no unpaired electron. Then, if a $^3He^+$ ion is formed by ionization of the ^3He atom, the depolarization is induced as prescribed by Eq. (5). In the next step, the $^3He^+$ ion is inelastically excited or ionized by the plasma electrons. As discussed in Subset. 3.1.2, the cross sections of inelastic scattering for the $^3He^+$ ion by the low energy electron are much larger than the ionization cross section of the $^3He^+$ forming the $^3He^{2+}$ ion. Therefore, the $^3He^+$ ions may be excited many times before ionization. The excited $^3He^+$ ion quickly deexcites to the ground state of the $^3He^+$ ion by photon emission. During the deexcitation (photon emission) processes, a considerable amount of the electron polarization of the $^3He^+$ atom is lost due to the spin-flip of the electron of the $^3He^+$ ion as far as the external magnetic field is not strong enough to decouple the fine structure interactions of the excited $^3He^+$ ion. The necessary magnetic field to decouple the fine structure interactions of the $^3He^+$ ion is over 16 T[7]. This indicates that the decoupling of the fine structure interactions is practically impossible. In the above deexcitation processes, the nuclear polarization of the $^3He^+$ ion may be depolarized as a result of the electron spin flip through the hyperfine interactions of the ^3He ion in the excited states. Fortunately, since the hyperfine interactions of the excited $^3He^+$ ion are much smaller than that of the ground state, the nuclear polarization is unperturbed by the unpaired electron of the $^3He^+$ ion during the deexcitation processes. However, once the excited $^3He^+$ ion reaches the ground state of the $^3He^+$ ion, the nuclear polarization is reduced by the presence of the strong hyperfine interactions. The nuclear polarization, P_{1e} decreased by

this effect is given by

$$P_{1e} = 1 - \frac{1}{2(1+x^2)}. \tag{6}$$

This equation is completely identical to Eq. (5). As stated above, since the inelastic cross section is far larger than the ionization cross sections, the inelastic scattering may be repeated many times before ionization, which may give rise to serious depolarization.

On the other hand, since the hydrogen atom is not confined in the ECR plasma because of neutrality of the hydrogen atom, the effect induced by the inelastic scattering can be basically ignored, which makes the proton polarization free from the depolarization due to the inelastic scattering.

When the $^3He^{2+}$ ion is formed by ionization of the $^3He^+$ ion in the ECR plasma, the depolarization no longer occurs because the $^3He^{2+}$ ion has no electron. However, if an ion confinement time is long enough to allow the de-ionization (electron recombination) processes expressed by Eq. (3),(4), further depolarizations are induced when the $^3He^+$ ion and ^3He atom in the $^3S_1$ state are formed, because the both states have unpaired electron(s). The polarization resulting from the former case is given also by Eq. (5), while the equation for the latter case is similar but with a somewhat smaller value of B_c , i.e., $B_c = 239$ mT [8].

If the ion confinement time is still remaining, an additional depolarization is expected whenever ionization and de-ionization processes include a $^3He^+$ ion as an intermediate step. Further, this cycle is repeated until the end of ion confinement time, and eventually the nuclear polarization is reduced. In particular, such processes may dominate using at the ECR-ionizer operated at high frequencies, in which the ion confinement time is long.

Contrary to the $^3He^{2+}$ case, the depolarization mechanism for the proton is much simpler: Since both the hyperfine interactions of the hydrogen atom are far smaller than those of the $^3He^+$ ion, the hyperfine decoupling of the hydrogen is almost realized even with a conventional low frequency ECR-ionizer, which indicates that the nuclear depolarization of the hydrogen is less pronounced. In addition, the $^3He^{2+}$ ion is depolarized twice during one cycle of ionization and de-ionization processes, whereas the proton experiences only one depolarization. This is a part of the reason why the proton depolarization is smaller than the $^3He^{2+}$ case. More decisive difference in the depolarization mechanism between the hydrogen and ^3He caused by the ESR (electron spin resonance) is discussed in the next subsection.

2.3 Depolarization due to the ESR (Electron Spin Resonance) transitions

Further depolarizations of the $^3He^+$ ion can be induced by the ECR microwaves in addition to the depolarizations mentioned in the previous subsection. The ESR (Electron Spin Resonance) transitions could be caused by the ECR microwave itself. This is because the ECR frequency is approximately equal to the ESR frequency due to the fact that the electron g-factor is nearly 2.

In fact, influence of the ESR on the proton polarization was carefully considered by Clegg et al.[4]. They concluded that a typical microwave power of ECR-ionizer ($\sim$ 50 W) was not so strong to reverse the electron spin by the following reason.: The ECR (ESR) resonance region has a thickness of 1.0×10^{-3} (cm) corresponding to the spatial region where the axial B-field is within one line width $\Delta\omega/(2\pi\gamma_J)$. Each hydrogen atom moves with a thermal motion in the ECR region. Therefore, the hydrogen atom does not spend a time longer than 3 ns in this resonance region. It is, consequently, difficult that the ESR makes the electron spin reverse in this short time. In addition, they claimed that even if the electron spin is reversed, the proton polarization is not reduced because of the presence of the strong decoupling field, i.e. a large x for Eq. (5).

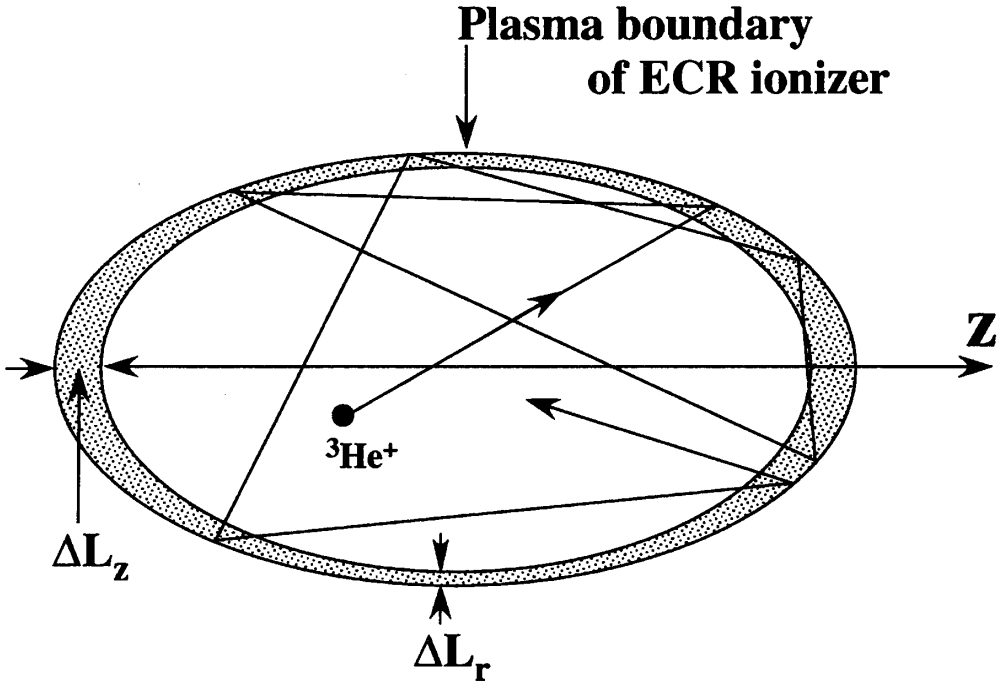

Fig. 1. Trajectory of the $^3He^+$ ion confined in the ECR plasma. The ion is reflected by the plasma wall and passes through the thin ESR regions where the ESR transitions occur. Note that a thickness of the ESR region in the z-direction is larger than that in the r-direction due to difference of the magnetic field inhomogeneities in these directions.

On the contrary, the above aspect should greatly be changed for the $^3He^+$ ion.

Firstly, the hyperfine interaction of the $^3He^+$ ion is not decoupled by the low magnetic field ($\sim$ 100 mT) of the ECR ionizer used for the hydrogen. As a result, the ^3He nuclear spin can be flipped in accordance with the spin flip of the electron of $^3He^+$ ion. Secondly, differing from behavior of the hydrogen atom, the $^3He^+$ ion is confined in the ECR plasma for a period of the ion confinement time, T_{ion}. Since a typical T_{ion} is 1$\sim$ 10 ms depending on the ECR magnetic field as discussed in Subsec. 3.2, the $^3He^+$ ion with a few eV bounces off the plasma wall many times within a period of T_{ion} as shown in Fig.1. The $^3He^+$ ion is exposed to the resonance microwave of the ECR (ESR) at every reflection during a time

$$\Delta t = \frac{\Delta L^{eff}}{v}, \tag{7}$$

where ΔL^{eff} is an effective thickness of the ESR resonance region as discussed in Appendix B, and v_{ion} is a $^3He^+$ ion velocity. The precession angle of the electron spin during this time period is given by

$$\Delta\theta = \gamma_J B_1 \Delta t, \tag{8}$$

where γ_J is the gyromagnetic ratio of the electron, B_1 is an amplitude of the magnetic field of the ECR (ESR) resonance microwave. The number of times N that the $^3He^+$ ion is reflected within the ion confinement time is given by

$$N = \frac{vT_{ion}}{L_{plasma}}, \tag{9}$$

where L_{plasma} is an average length of the ECR plasma. Consequently, the integrated precession angle of the electron spin during the ion confinement time is obtained by

$$\Theta = \Delta\theta\sqrt{N}. \tag{10}$$

The reason why Θ is proportional not to N but to $\sqrt{N}$ is as follows: The direction of B_1 field and phase of the precession angle are randomly oriented for each ESR transition caused at bouncing of the $^3He^+$ ion on the plasma wall. Therefore, the integrated precession angle does not follow a simple sum-up of $\Delta\theta$ but follows the principle of the random walk as mentioned by Cates et al.[9]. As demonstrated in Appendix B, the integrated precession angle of the electron spin Θ is estimated to be 2.7 radian for the 14.5 GHz ECR ionizer operated with a microwave power of 500 W, where the ion confinement time is assumed to be 1 ms. This suggests the ESR effect is significant, which eventually induces the nuclear depolarization as well. More specifically, the

transitions denoted by ① ↔ ③, and ② ↔ ④, in ref. [10] induce the spin-flip of both the electron and nucleus as far as the external field, B is not strong enough to decouple the hyperfine interaction.

On the basis of the formalism of Ohlsen[10] the polarization due to the ESR transition is given by

$$P_{ESR} = \frac{|x|}{\sqrt{1+x^2}}. \tag{11}$$

3 Numerical calculations

In the first part of this section, we give parameters necessary for the Monte Carlo simulation applied to calculate the polarization of $^3He^{2+}$ ion and proton produced in the ECR-ionizer. In the latter part of this section, an outline of the Monte Carlo simulation is presented.

3.1 Ionization and De-ionization rates

H^+, $R(^3He)_{01}$ for $^3He \rightarrow {}^3He^+$, and $R(^3He)_{12}$ for $^3He^+ \rightarrow {}^3He^{2+}$ are, respectively, expressed by

$$R_{01}(H) = n_e \sigma_{0\rightarrow 1}(H) \times v_e, \tag{12}$$

$$R_{01}(^3He) = n_e \sigma_{0\rightarrow 1}(^3He) \times v_e, \tag{13}$$

$$R_{12}(^3He) = n_e \sigma_{1\rightarrow 2}(^3He) \times v_e, \tag{14}$$

where n_e is an electron density ($1/cm^3$), v_e is an electron velocity (cm/s), σ's are ionization cross sections (cm^2) for the hydrogen and ^3He , and an suffix, $i \rightarrow i+1$ corresponds to the ion change of charge state from i to $i+1$. Assuming that n_e in the ECR plasma is equal to the critical density, n_e[6] is expressed by

$$n_e = \left(\frac{f_{ECR}}{8980}\right)^2, \tag{15}$$

where f_{ECR} is an ECR frequency (Hz)[6]. A value of $\sigma \times v_e$ averaged over the Maxwellian electron distribution in the ECR plasma can be evaluated by using an empirical formula of Lotz[11] as expressed by

$$< \sigma v_e > = 6.7 \times 10^{-7} \times \sum_{k=1}^{N} \frac{a_k q_k}{T^{\frac{3}{2}}} \times \left\{ \frac{1}{P_k/T} \int_{P_k/T}^{\infty} \frac{e^{-x}}{x} dx - \frac{b_k e^{c_k}}{P_k/T + c_k} \int_{P_k/T+c_k}^{\infty} \frac{e^{-y}}{y} dy \right\} \qquad (16)$$

where P_k is the binding energy (eV) of electrons in the k-th subshell, T is the electron temperature (eV), q_k the number of equivalent electrons in the k-th subshell, a_k,b_k, c_k are individual constants (in a unit of 10^{-14} cm^2eV^2). Here, their numerical values are,respectively, summarized as follows; for ^3He , P_1=24.6, a_1=4.0, b_1=0.75, c_1=0.46, for $^3He^+$, P_1=54.4, a_1=4.4, b_1=0.38, c_1=0.60, and for H, P_1=13.6, a_1=4.0, b_1=0.60, c_1=0.56, where only k=1 is valid for H, ^3He , and $^3He^+$. In Fig. 2, the ionization rates (cm^3/s) thus

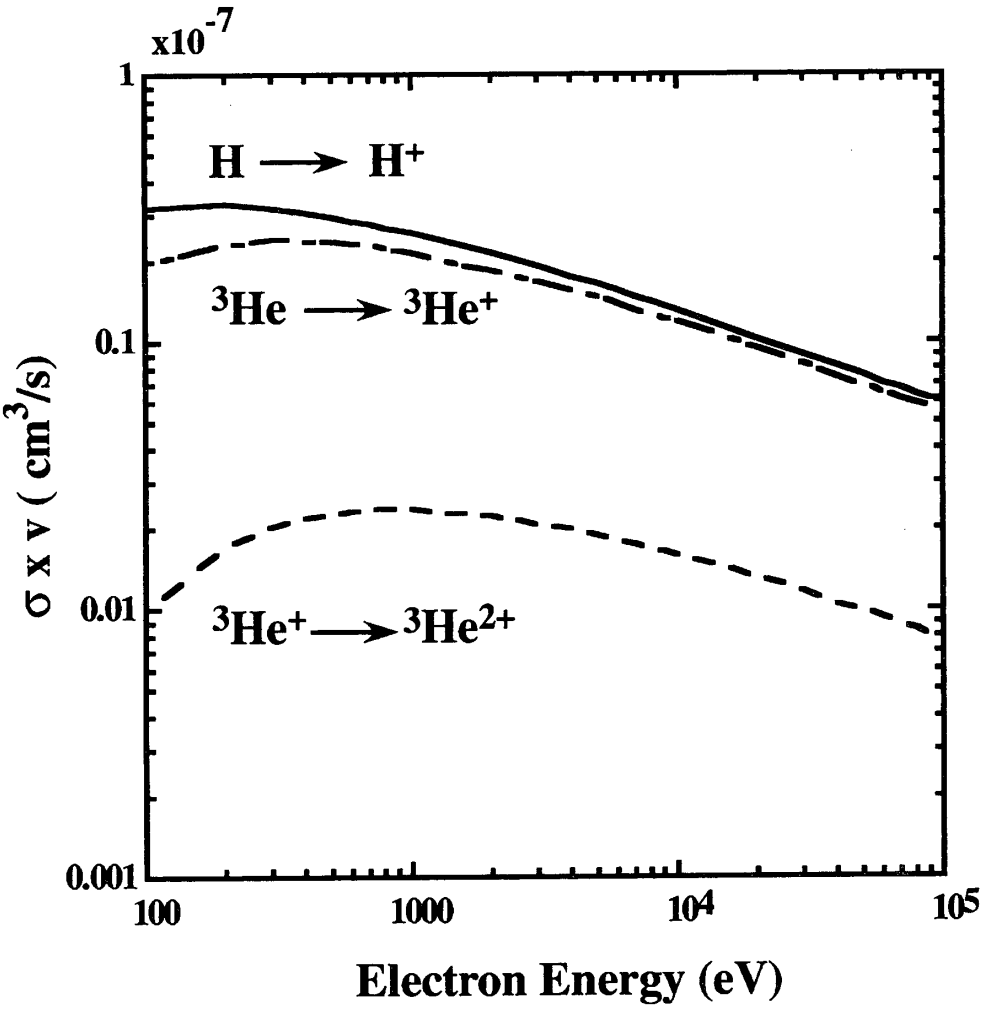

Fig. 2. Ionization rates for hydrogen and ^3He in case of electron bombardment

obtained are plotted for H, ^3He , and $^3He^+$. From Fig. 2, we take the following values assuming that a mean electron temperature is 500 eV; $< \sigma_{0\to1}(H) \times v_e >= 2.9 \times 10^{-8}$, $< \sigma_{0\to1}(^3He) \times v_e >= 2.5 \times 10^{-8}$, and $< \sigma_{1\to2}(^3He) \times v_e >= 0.23 \times 10^{-8}$.

3.1.2 Inelastic scattering of $^3He^+$

As discussed in the previous section, inelastic scatterings of $^3He^+$ ion by the electron in the ECR plasma are one of the important processes causing the $^3He^{2+}$ depolarization. In this subsection, we estimate the energy dependence of the total cross sections for inelastic scattering of the $^3He^+$ ion by using an empirical rule[12] and the AMDIS-IAEA Database[13].

The empirical formalism[12] of inelastic scattering cross sections valid for the hydrogen-like atoms and ions is expressed by

$$\sigma_{n\to n'} = k\frac{\pi a_0^2}{z^4} n^7 \sqrt{n'}[n'^2 - n^2]^{-2}\frac{F(x)}{x}, \tag{17}$$

where k is a normalization constant, x is $\epsilon_e/E_{nn'}$, ϵ_e is the electron kinetic energy, $E_{nn'}$ is the transition energy (=$13.6/z^2[n^{-2} - n'^{-2}]$ (eV)), a_0 is the Bohr radius (=0.529×10^{-8} cm), z is a nuclear charge, n, n' are the principal quantum numbers of the initial and final state, and F(x) is given by

$$F(x) = 14.5ln(x) + 4.15 + 9.15x^{-1} + 11.9x^{-2} - 5.16x^{-3}. \tag{18}$$

The normalization constant k is determined to be k = 1.37 by comparing the sum of the observed inelastic cross sections from the 1s to 2s and 2p states (=2.45×10^{-18} cm^2 at 1 keV[13]).

We define the total inelastic cross section σ_{ex} as a sum of the inelastic cross sections given by Eq. (17) up to n' = 100 with n =1. Then, we obtain the total inelastic scattering rate defined by

$$R_{ex} = \sigma_{ex} \times v_e, \tag{19}$$

where v_e is the electron kinetic energy. The calculated results are demonstrated in Fig. 3, where the ionization rates for the $^3He^+$ to $^3He^{2+}$ ions are also presented as a guide of reference. It is remarkable that the inelastic scattering rate for the $^3He^+$ ion is almost one order of magnitude larger than the ionization rate as long as the electron kinetic energy is less than 500 eV. This implies that a significant depolarization may be caused by the repetitive inelastic scatterings before the ionization with low energy electrons.

3.1.3 De-ionization (Electron Recombination) Rates

De-ionization (electron recombination) processes occurring in the ECR-ionizer are generated by collisions of produced ions with residual gases in the ECR plasma region. Similarly to the expression of ionization rates (see Eq. (12)~(14)),

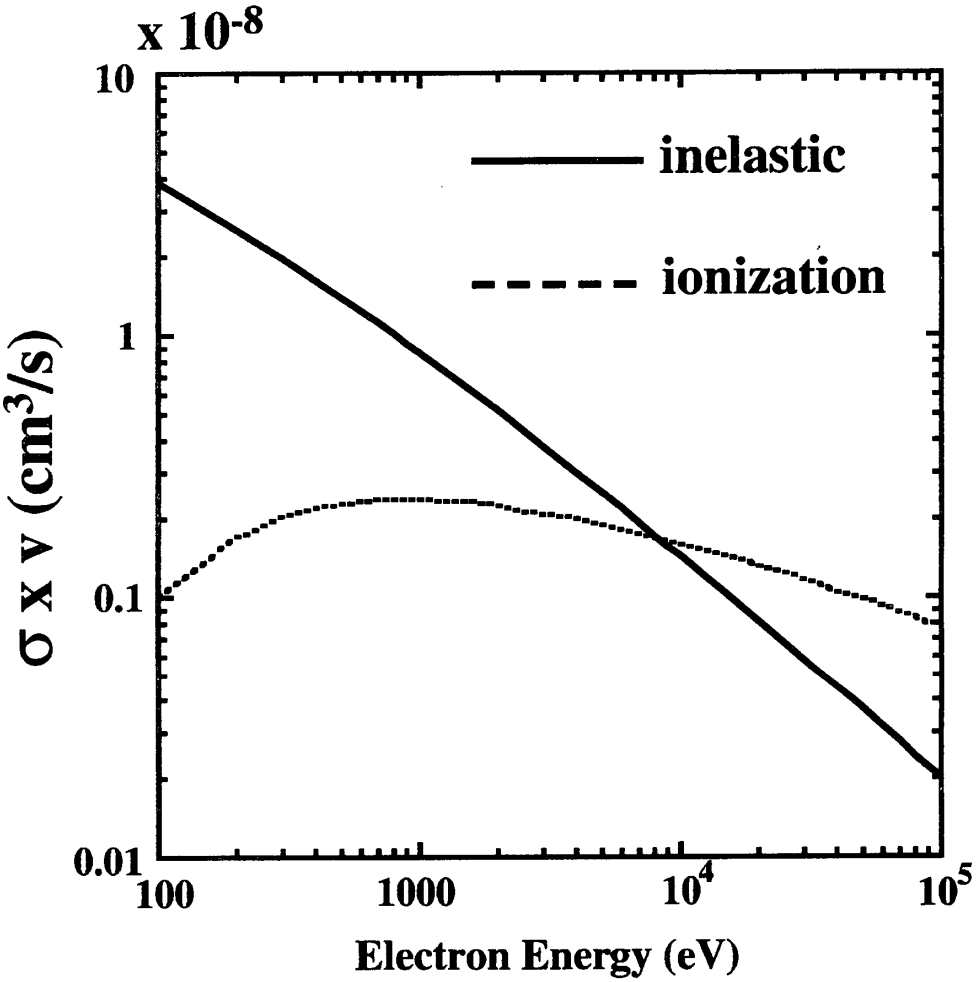

Fig. 3. Inelastic scattering rate for the $^3He^+$ ion

the de-ionization rates (cm^3/s) for proton, $^3He^+$, and $^3He^{2+}$ are, respectively, defined by;

$$R_{10}(H) = n_a \sigma_{1\to 0}(H) \times v_{ion}, \tag{20}$$

$$R_{10}(^3He) = n_a \sigma_{1\to 0}(^3He) \times v_{ion}, \tag{21}$$

$$R_{21}(^3He) = n_a \sigma_{2\to 1}(^3He) \times v_{ion}, \tag{22}$$

where n_a is a residual gas density ($1/cm^3$), and v_{ion} is an ion velocity(cm/s). Here, a reasonable value of n_a is evaluated from our past experience on the ECR ion sources operated at 2.45 GHz and 10 GHz according as the following procedures: The measured gas flow rates, 0.1 cc/min. for the ECR-ionizer operated at 2.45 GHz[14], and 0.06 cc/min. for that operated at 10 GHz[7] correspond to the gas pressure of the ECR plasma region, $P_a = 3 \sim 5 \times 10^{-5}$ Torr., assuming reasonable values for a pumping speed and gas flow conductance. From the gas pressures, n_a can be obtained as

$$n_a = (1.1 \sim 1.8) \times 10^{12} \tag{23}$$

In the present Monte Carlo simulation, we vary P_a in a broad range from 5×10^{-5} to 1.0×10^{-6} Torr.. Regarding the ion velocity, it is supposed that the ion temperature is believed that it is never higher than 10 eV . In our case, we assume 5 eV for ^{3}He and 3 eV for hydrogen, respectively. The de-ionization cross sections are referred from an empirical formula of Müller and Salzborn [15]. The cross section of de-ionizations from the charge state i to the charge state $i-1$ is given by

$$\sigma_{i\to i-1} = 1.43\times 10^{-12} i^{1.17} V_{0\to 1}^{-2.76}, \tag{24}$$

where $V_{0\to 1}$ is an ionization potential for a neutral atom; 24.6 eV for ^{3}He , and 13.6 eV for hydrogen. Assuming that the residual gases are only ^{3}He and hydrogen, we can obtain the de-ionization cross sections for the $^3He^{2+}$, $^3He^{+}$ and proton, respectively as shown below;

$$\begin{aligned}
\sigma_{2\to 1}(^3He) &= 4.66\times 10^{-16},\\
\sigma_{1\to 0}(^3He) &= 2.07\times 10^{-16},\\
\sigma_{1\to 0}(H\ \ ) &= 10.6\times 10^{-16}.
\end{aligned} \tag{25}$$

As an additional de-ionization process, we consider the symmetric resonant charge transfer process expressed by

$$^3He^{2+} + {}^3He \longrightarrow {}^3He + {}^3He^{2+}, \tag{26}$$

The cross section of this process σ_{double} is estimated from the total cross section for the $^4He^{2+} + {}^3He$ system measured in a $^4He^{2+}$ impact energy range from 50 to 540 eV[16]. σ_{double} at 5 eV $^3He^{2+}$ energy is obtained by extrapolating the data at a ^{4}He energy higher than 50 eV in ref. [16] to the low energy limit;

$$\sigma_{double} \sim 7\times 10^{-16}. \tag{27}$$

The above value is comparable or somewhat larger than those of Eq. (25), i.e., the single de-ionization cross sections.

3.2 Ion confinement time

An ion confinement time, T_{ion} is a period during which ions are confined in the ECR plasma. This parameter plays an important role in determining the final $^3He^{2+}$ polarization because the parameter is associated with the number of times that the ionization and de-ionization is repeated. Since there has

been no reliable data compilation of the ion confinement time, we use the speculation of Geller[5] as described by

$$T_{ion} = \tau_{ion} \times \left(\frac{f_{ECR}}{10} \right)^{1.5}, \tag{28}$$

where f_{ECR} is an ECR frequency (GHz), a coefficient, τ_{ion} is an ion confinement time (s) at f_{ECR} = 10 GHz. In the present calculation we employ τ_{ion} = 0.01~0.001 (s). Note that the time dependent measurement of the extracted heavy ion currents from the 10 GHz ECR ion source at ANL[17] suggested a longer ion confinement time. In our calculation, we do not take the change of the ion confinement time according to the ion charge state.

Finally, we define R_{ion} by

$$R_{ion} = \frac{1}{T_{ion}}. \tag{29}$$

This is a parameter corresponding to the rate of ion released from the plasma region.

3.3 Monte Carlo simulation

We present an outline of the Monte Carlo simulation applied to calculate the $^3He^{2+}$ and proton polarizations resulting from multiple ionization and de-ionization processes occurring in the ECR plasma during the ion confinement times. Schematic diagrams showing the Monte Carlo simulation applied to the $^3He^{2+}$ and proton polarizations are illustrated in Fig. 4. We start with injection of a nuclear-polarized ^3He atom into the ECR plasma (see Fig. 4-a)). This atom, then, becomes a $^3He^+$ ion with an ionization rate, R_{01} (^3He) or exits from the ECR plasma region. Since there is no chance for a ^3He atom to be ionized outside the ECR plasma region, we define an effective plasma length, L_{eff}, within which a ^3He atom is ionized. L_{eff} should not be an actual dimension of the plasma length, L_{plasma}, but should be

$$L_{eff} = L_{plasma} \times N, \tag{30}$$

where N is a number/s that the ^3He atom traverses the plasma region owing to the wall scatterings of the ECR chamber. Though it is a difficult task to determine L_{eff} and N, we tentatively take L_{eff} = 50 cm assuming that L_{plasma}=5cm and N=10.

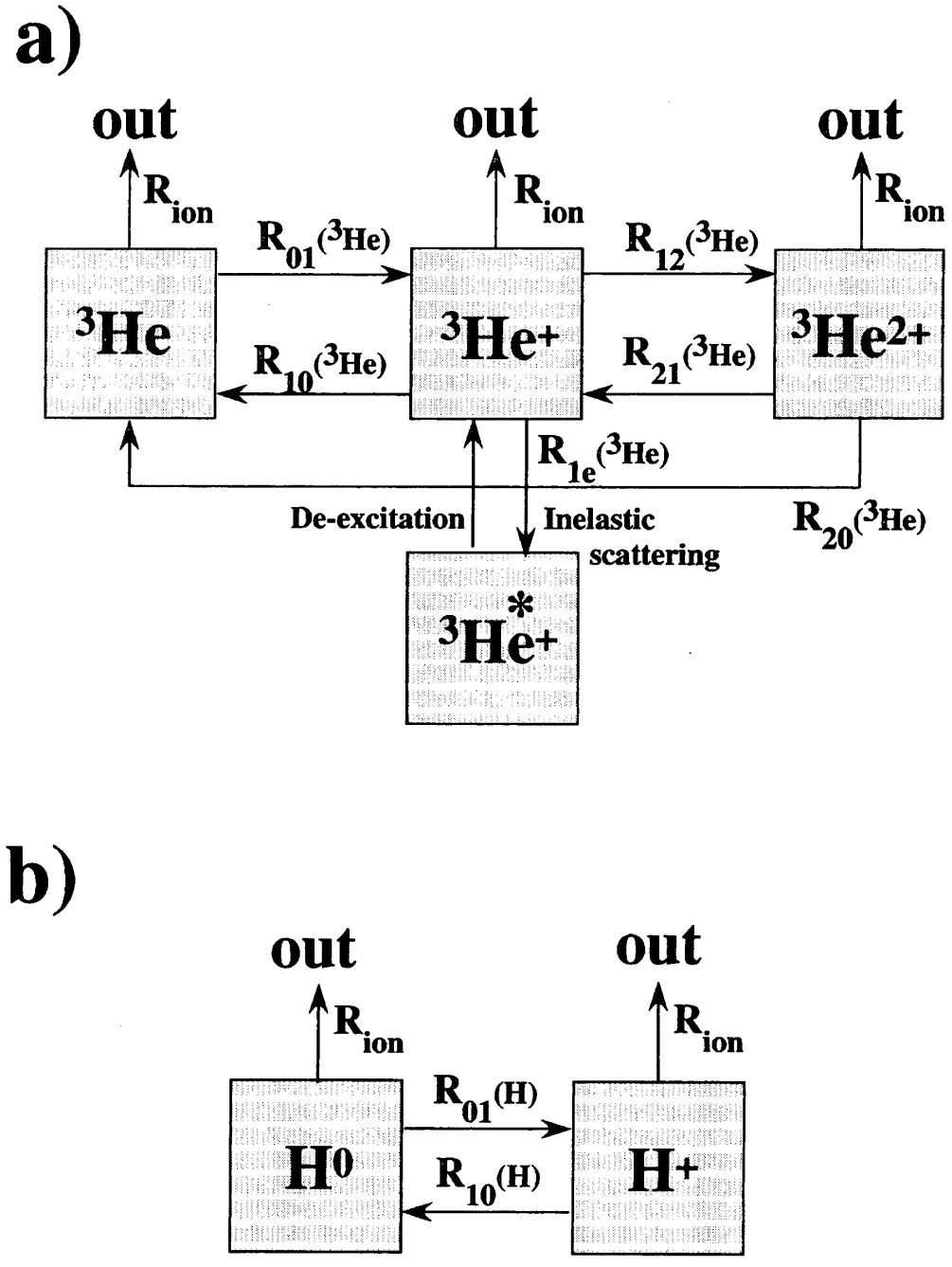

Fig. 4. Schematic pictures showing the physical processes in the ECR ionizer for the Monte Carlo Simulation. a) for ionization of ^{3}He , and b) for ionization of the hydrogen. See the text for symbols used in this picture.

When the ^{3}He atom changes to a $^3He^+$ ion by ionization, the depolarization is determined by Eq. (5) and Eq. (11). The produced $^3He^+$ ion, then, evolves via following four routes;

(1) quitting the plasma region and extracted as a $^3He^+$ ion beam with a rate, R_{ion},
(2) returning to the neutral ^{3}He with a de-ionization rate, $R_{10}(^3\mathrm{He})$,
(3) inelastic scatterings and subsequent deexcitations with a rate, R_{1e},
(4) becoming a $^3He^{2+}$ ion with an ionization rate, $R_{12}(^3\mathrm{He})$.

If the $^3He^+$ ion returns to the neural ^3He atom in the $^3S_1$ state, there exists a further depolarization expressed by an equation similar to Eq. (5), where x is modified by the hyperfine interaction of the ^3He $^3S_1$ state having unpaired electrons. Since the de-ionization processes to the non-depolarizing component, i.e., the $^1S_1$ state of ^3He atom is expected to be only 1/4 of the total de-ionization processes, we neglect formation of the $^1S_1$ state. If the $^3He^+$ ion is excited and subsequently deexcited to the ground state again, the depolarization is induced as prescribed by Eq. (6). Since the cross section of the inelastic scattering is far larger than that of the ionization, the inelastic scattering processes are repeated many times before ionization. Thereafter, if the $^3He^+$ ion is ionized to a $^3He^{2+}$ ion, then, there is no further depolarization. The generated $^3He^{2+}$ ion thus formed further evolves via the following three routes if the ion confinement time is long enough,

(1) returning to the $^3He^+$ ion (de-ionization),
(2) returning to the ^3He atom (symmetric resonant charge transfer),
(3) going out of the plasma region and is extracted as a polarized $^3He^{2+}$ ion beam.

If the $^3He^{2+}$ ion is de-ionized and becomes the $^3He^+$ ion, there exists a depolarization prescribed by Eq. (5) and Eq. (11). Then the de-ionized $^3He^+$ ion further evolves according to the scheme shown in Fig. 4. If the $^3He^{2+}$ ion is de-ionized to ^3He by the symmetric resonant charge transfer processes, the depolarization is described by Eq. (5) and Eq. (11) The present Monte Carlo simulation takes all the processes mentioned above in order to calculate the $^3He^{2+}$ polarization. In the present work, trial atoms are generated 10^5 times/run and the ^3He nuclear polarization is calculated by recording an individual trajectory of the trial atoms.

The Monte Carlo simulation is similarly applied to the proton case as shown in Fig. 4-b). Since the contributing states are only a neutral hydrogen atom and proton, the calculation becomes much more simpler.

Finally, we summarize the parameters employed in the present Monte Carlo simulation; the ion temperature is 5 eV for ^3He and 3 eV for hydrogen, the electron temperature is 500 eV for ^3He and 1000 eV for hydrogen, respectively, $\tau_{ion} = 1 \sim 10$ ms (Eq. 28), and the gas pressure is varied from 5×10^{-5} to 1×10^{-6} Torr. for ^3He and from 5×10^{-5} to 5×10^{-6} Torr. for hydrogen.

4 Calculated results and discussion

4.1 Ratios of $^3He^{2+}$ to $^3He^+$ ion currents

In this subsection, reliability concerning how well the Monte Carlo simulation calculates physical quantities. For this purpose, we compare the calculated results with the experimentally observed ratios of $^3He^{2+}$ to $^3He^+$ ion currents extracted from the ECR ionizers. This is shown in Fig. 5. The ratios are plotted

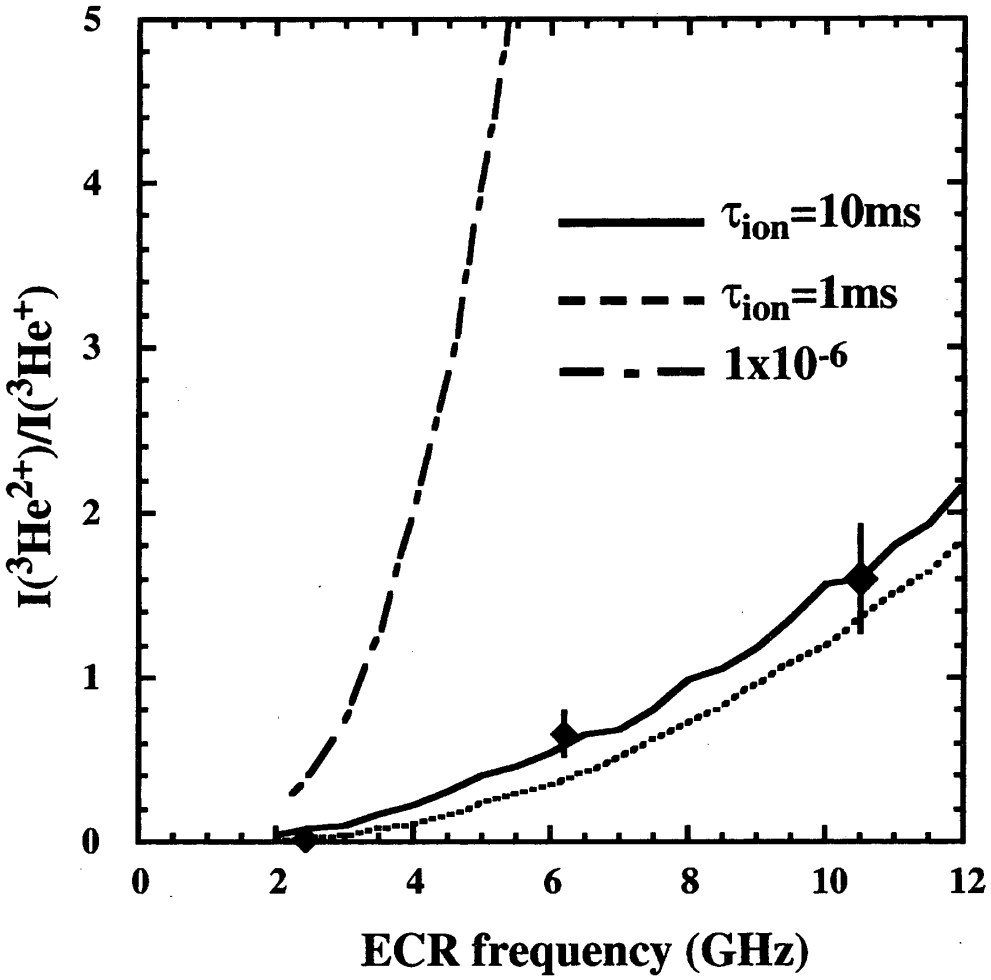

Fig. 5. Ion current ratios, $I(^3He^{2+})/I(^3He^+)$ extracted from the ECR ionizers. The closed diamonds are the experimental data, and curves are the results of the Monte Carlo simulation. See the text for further details.

as a function of f_{ECR}, where the closed diamonds are the experimental results [6,7,14], the solid curve is the calculated results with τ_{ion} =10 ms and the gas pressure, P_a= 5 × 10^{-5} Torr., the dotted curve is the calculated results with τ_{ion} =1 ms and P_a=5 × 10^{-5} Torr., and the dash-dotted curve is the calculated results with τ_{ion} =10 ms and P_a=1 × 10^{-6} Torr., respectively. Interestingly, the ratios are less sensitive to the ion confinement time, while very sensitive to the gas pressure. This suggests that lowering the residual gas pressure is

very important for obtaining the more $^3He^{2+}$ ion, which is a widely accepted idea of the ECR-ionizer. It is remarkable that not only the increasing trend but also absolute values for the experimental results are well reproduced by the present Monte Carlo simulation with a reasonable parameter set. From this result, the present calculation may also provide the $^3He^{2+}$ polarization correctly.

4.2 Calculated Polarizations

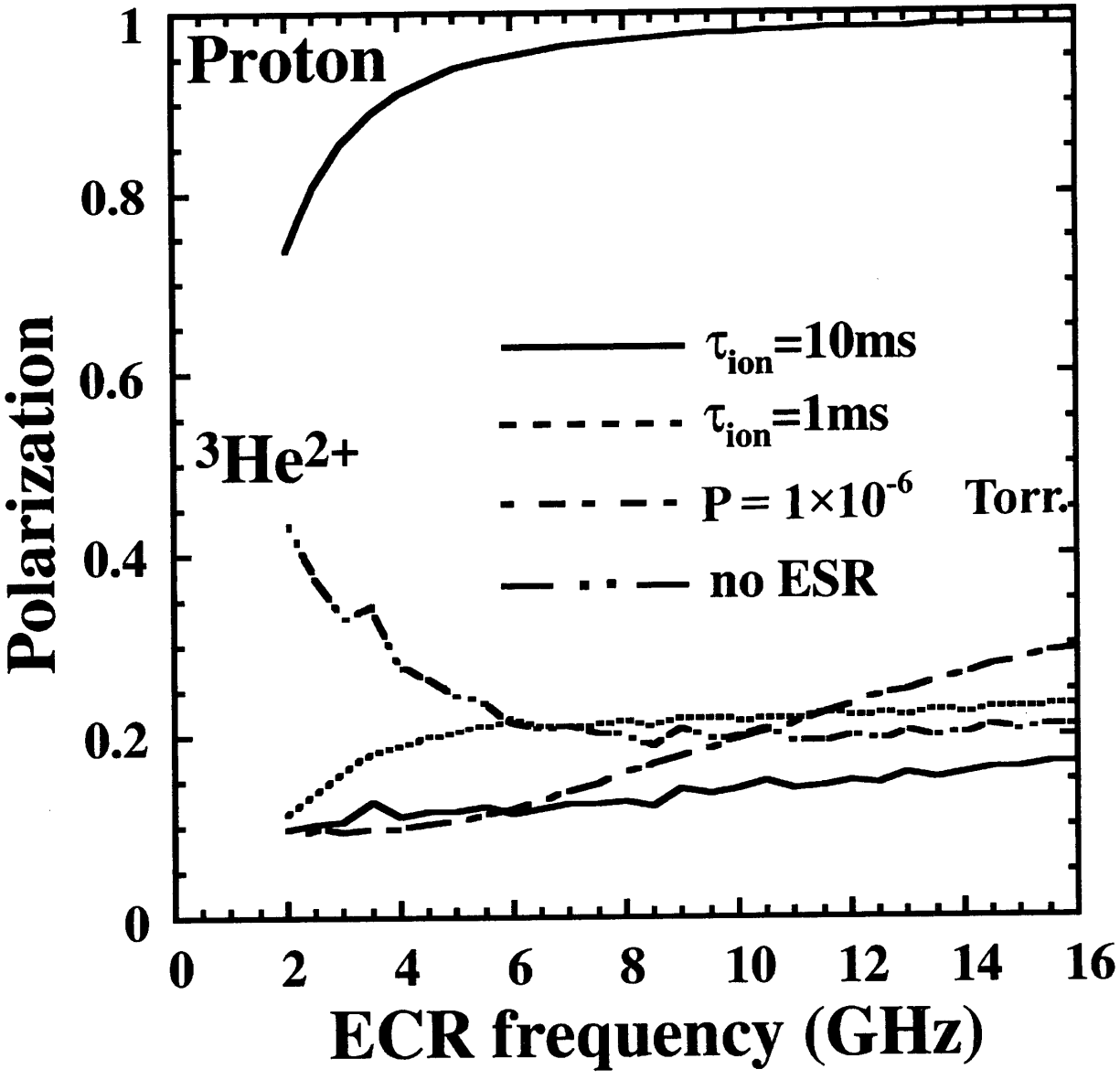

Fig. 6. $^3He^{2+}$ and proton polarizations plotted as a function of ECR frequency (GHz). See the text for further details.

The results of the ^3He nuclear polarization are compared with those of the proton polarization. To simplify the discussion, we assume that both the ^3He and hydrogen gases are fully polarized, i.e., P_0 =1.0. In Fig. 6, the calculated po-

larizations for $^3He^{2+}$ ion and proton are plotted as a function of f_{ECR} with various parameter sets. The solid, dotted, dot-dashed, and double-dot-dashed curves (lower curves) are,respectively, the results of the $^3He^{2+}$ polarization, and the solid curve (upper curve) is the results of the proton polarization. The solid curve is the calculated results with τ_{ion} = 10 ms and the gas pressure, $P_a = 5 \times 10^{-5}$ Torr., the dotted curve is the calculated results with τ_{ion} = 1 ms and $P_a = 5 \times 10^{-5}$ Torr., the dot-dashed curve is the calculated results with τ_{ion} =10 ms and $P_a = 1 \times 10^{-6}$ Torr., and the double-dot-dashed curve is the calculated results with τ_{ion} =10 ms and $P_a = 5 \times 10^{-5}$ Torr. with the ESR effect switched off, respectively. The upper solid curve shows the results of the proton polarization with τ_{ion} =10 ms and P_a in a range varied from 5×10^{-5} to 5×10^{-6} Torr. Differing from the behavior of ^3He , the gas pressure does not significantly affect on the proton polarization.

At first glance, there exists a strikingly difference between the $^3He^{2+}$ and proton polarizations; the proton polarization is close to the hydrogen gas polarization, i.e., P_0 =1.0 particularly at high ECR frequencies, while the $^3He^{2+}$ polarization is greatly reduced in comparison with the initial ^3He gas polarization. Intuitively, this difference is understood as follows: The $^3He^+$ ion confined in the plasma for a long time is depolarized due to an unpaired electron of the $^3He^+$ ion, while the proton confined in the plasma is not depolarized due to absence of an unpaired electron. In addition, though the hydrogen atom with an unpaired electron has a chance to be depolarized, the depolarization is expected to be negligibly small because it is not confined in the plasma.

Next, we move to the discussion on the change of the $^3He^{2+}$ polarizations as a function of the ECR frequency. Looking at the solid curve in Fig. 6, the $^3He^{2+}$ polarization is almost constant with a slow increase according as an increase of the ECR frequency. This tendency is qualitatively understood as follows: In the low ECR frequency region, the $^3He^{2+}$ polarization is mainly determined by the depolarization due to smallness of the hyperfine decoupling field, while at the high ECR frequency region, an additional depolarization due to the ESR transitions, the multiple ionizations, inelastic scatterings and de-ionization processes are predominated as a result of longer ion confinement times. The depolarization due to the ion confinement is more clearly shown in the dotted curve in Fig. 6, where the polarization is increased as a result of shorter ion confinement time.

The effect of the residual gas is very important as demonstrated in Fig. 6. When the residual gas pressure is 1.0×10^{-6} Torr., the polarization (the dotted-dashed curve) is rapidly increased according as an increase of the ECR frequency and the polarization reaches at 0.3. This is a simple consequence of the decrease of the multiple ionization and de-ionization processes.

Finally, we mention the effect of the ESR transitions. As discussed previous

sections, the ESR transition is valid only for a long ion confinement time. Therefore, the depolarization due to the ESR transitions would become less pronounced at the low ECR frequency region. We plot the results with the ESR switched off. This is shown as the double-dot-dashed curve in Fig. 6. At the low frequency region, the polarization is quickly increased, while at the higher ECR frequency region, there is no improvement of the polarization compared with the condition that the ESR transitions are present, though the polarization is somewhat larger than that with the ESR transitions. This result suggests that at the low ECR frequency region the ESR effect is the major origin of the depolarization if it really exists, while at the higher ECR frequency region the ESR effect becomes less important, i.e. the depolarizations due to the multiple ionization and de-ionization becomes predominated.

4.3 Practical value of the ^{3}He polarization

In this subsection, we speculate upon the value of ^{3}He polarization expected by means of the ECR-ionizer with ^{3}He gas with polarization practically available. Nowadays the ECR-ionizer applied for the polarized hydrogen and deuteron is regarded as a well established technique. Fully polarized hydrogen is produced by the atomic beam method and the proton beam whose polarization is over 0.75 is injected to the cyclotron without serious problem.

On the other hand, the status of the ECR-ionizer applied for ionization of the ^{3}He gas is quite different. According to the latest record on the ^{3}He gas polarization produced by the direct optical pumping of ^{3}He gas, the maximum polarization obtained by the Mainz group is $\sim$ 0.8[18]. But, since this record could be achieved only through sophisticated technology by the experts, we employ a well-established world standard value, $\sim$ 0.5 [19]. Using the solid curve in Fig. 6 and the ^{3}He gas polarization of 0.5, it is significantly difficult to get the $^3He^{2+}$ ion beam with the polarization larger than 0.2, though the $^3He^{2+}$ beam current larger than 100 μA is practically available.

5 Conclusion and future outlook

A Monte Carlo simulation was performed to calculate the $^3He^{2+}$ and proton polarizations obtained by ionizing polarized ^{3}He and hydrogen gases with ECR ionizers. The varied range of the ECR frequency was from 2 to 16 GHz. It was found that the depolarization of protons was less significant in all the ECR frequency range studied, while that of $^3He^{2+}$ was surprisingly large. The origin of the large $^3He^{2+}$ depolarization is due to the large hyperfine and fine structure interactions of $^3He^+$ ion. As a result, multiple ionization, inelastic

scattering, and deionization of ^3He atom and ions play a substantial role in producing the unexpectedly large $^3He^{2+}$ depolarization.

With a polarized ^3He gas currently available, ~ 0.5, it was very difficult to obtain the $^3He^{2+}$ polarized beam over 0.2.

In conclusion, though the ECR-ionizer is quite effective in extracting a polarized proton beam, we must be prudent in extrapolating this method to the polarized^3He ion source.

Acknowledgments

One of authors (M.T.) greatly acknowledges Prof. Sakemi and Prof. Tamii for their sincere discussion on the ESR transitions and inelastic scattering of $^3He^+$ ions. We are also indebt to the director of RCNP, Osaka University, Prof. Toki for his encouragement. We are deeply indebted to Prof. Greenfield, Prof. Fujiwara, Dr. Matsuoka, Dr. Yosoi, and Dr. Takahisa for their critical reading of our manuscript, invaluable suggestions and deep understanding of this subject.

References

[1] S. D. Baker, E.B. Carter, D. O. Findley, L. L. Hatfield, G. C. Philips, N. D. Stockwell and G. K. Walters, Phys. Rev. Lett. **20** (1968) 738 and 1020 (E).

[2] M. Tanaka, Proceedings of the International Workshop on Polarized ^3He Ion Sources and Gas Targets and Their Applications, Oppenheim, Germany 2002, MON-11.

[3] AIP Conference Proceedings 293, 1993, Madison, U.S.A. ed. L.W. Anderson and W. Haeberli, p.65.

[4] T.B. Clegg, V. König, P.A. Schmelzbach, and W. Gr*ddotu*ebler, Nucl. Instr. and Meth., **A238** (1985) 195.

[5] R. Geller, Ann. Rev. Nucl. Part. Sci. **40** (1990) 15.

[6] Y. Jongen, and C.M. Leineis, "The Physics and Technology of Ion Sources", ed. I.G. Brown, John Wiley & Sons, 1989, New York, Chichester, Brisbane, Toronto, and Singapore, p.207.

[7] M. Tanaka, N. Shimakura, T. Ohshima, K. Katori, M. Fujiwara, H. Ogata, and M. Kondo, Phys. Rev. **A50** (1994) 1184.

[8] P.J. Nacher, and M. Leduc, J. Physique **46** (1985) 2057.

[9] G.D. Cates, S.R. Schaefer, and W. Happer, Phys. Rev. **A37** (1988) 2877.

[10] G.G. Ohlsen, J.L. MckKibben, R.R. Stevens, Jr., and G.P. Lawrence, Nucl. Instr. and Meth. **73** (1969) 45.

[11] W. Lotz, Zeitschrift für Phys. **216** (1968) 241.

[12] V.I. Fisher, Yu. V. Ralchenko, V.A. Bernshtam, A. Goldgirsh, and Y. Maron, L.A. Vainshtein, I. Bray, and H. Golten, Phys. Rev. **A55** (1997) 329.

[13] http://www-amdis.iaea.org/

[14] M. Tanaka, T. Ohshima, K. Katori, M. Fujiwara, T. Itahashi, H. Ogata, M. Kondo, and L.W. Anderson, Nucl. Instr. and Meth. **A302** (1991) 460.

[15] A. Müller, and E. Salzborn, Phys. Lett. **62A** (1977) 391.

[16] H. Schrey, B. Huber, Z. Phys., **A273** (1975) 401.

[17] R.C. Pardo, R. Harkewicz, and P.J. Billquist, Rev. Sci. Instr. **67** (1996) 1602.

[18] Y. Sakemi, Private communication.

[19] E.W. Otten, Proceedings of the International Workshop on Polarized ^{3}He Ion Sources and Gas Targets and Their Applications, Oppenheim, Germany 2002, MON-03.

Depolarization for $^3He^+$ Ion

Suppose that just after 1-st ionization $^3He^+$ ions are in the ground state expressed by

$$\psi^+(^3He)\psi^-(e^-) + \psi^+(^3He)\psi^+(e^-), \qquad (A-1)$$

where $\psi^+(^3He)\psi^-(e^-)$ and $\psi^+(^3He)\psi^+(e^-)$ with equal probabilities. But the former state in Eq. (A-1) is not pure states listed by

$$\begin{aligned}
\Psi(1,\ 1) &= \psi^+(^3He)\psi^+(e^-),\\
\Psi(1,\ 0) &= \sin\beta\psi^-(^3He)\psi^+(e^-) + \cos\beta\psi^+(^3He)\psi^-(e^-),\\
\Psi(0,\ 0) &= \cos\beta\psi^-(^3He)\psi^+(e^-) - \sin\beta\psi^+(^3He)\psi^-(e^-),\\
\Psi(1,-1) &= \psi^-(^3He)\psi^-(e^-), \qquad (A-2)
\end{aligned}$$

where $\sin\beta = \sqrt{\frac{1+x/\sqrt{1+x^2}}{2}}$ and $\cos\beta = \sqrt{\frac{1-x/\sqrt{1+x^2}}{2}}$. Then, the former term in Eq. (A-1) evolves as

$$\begin{aligned}
\psi^+(^3He)\psi^-(e^-) \rightarrow\ & \cos\beta\Psi(1,0)exp[-iE(1,0)t/\hbar] - \sin\beta\Psi(0,0)exp\{-iE(0,0)t/\hbar\}\\
=\ & \cos\beta[\sin\beta\psi^-(^3He)\psi^+(e^-) + \cos\beta\psi^+(^3He)\psi^-(e^-)]\\
& \times exp(-iE(1,0)t/\hbar)\\
& - \sin\beta[\cos\beta\psi^-(^3He)\psi^+(e^-) - \sin\beta\psi^+(^3He)\psi^-(e^-)]\\
& \times exp(-iE(1,0)t/\hbar). \qquad (A-3)
\end{aligned}$$

Then, the probability to find the state $\psi^+(^3He)\psi^-(e^-)$ is given by

$$\begin{aligned}
&\frac{1}{2} \mid \cos^2\beta exp\{-iE(1,0)t/\hbar\} + \sin^2\beta exp\{-iE(0,0)t/\hbar\} \mid^2\\
&= \{1 - 2\sin^2\beta\cos^2\beta(1-\cos\Delta\omega t)\}/2\\
&= \frac{1}{2} - \frac{1}{2}\sin^2(\Delta\omega t/2)/(1+x^2) \qquad (A-4)
\end{aligned}$$

Then, the probability to find the state, $\psi^-(^3He)\psi^+(e^-)$ at time t is given by $\frac{1}{2}\sin^2(\Delta\omega t/2)/(1+x^2)$. Here, $\Delta\omega$ is given by

$$\Delta\omega = [E(0,0) - E(1,0)]/\hbar = \mid \Delta W\sqrt{1+x^2}/\hbar \mid \qquad (A-5)$$

where $\Delta W/\hbar$ = -8.67 GHz for $^3He^+$ ion. Adding the probability to find the state $\psi^+(^3He)\psi^+(e^-)$, the polarization, P of the $^3He^+$ ion is given by

$$P = \frac{1}{2} + \{\frac{1}{2} - \frac{1}{2}\sin^2(\Delta\omega t)/(1+x^2)\} - \frac{1}{2}\sin^2(\Delta\omega t)/(1+x^2)$$
$$= 1 - \sin^2(\Delta\omega t/2)/(1+x^2) \qquad (A-6)$$

After averaging over time t, the final polarization is

$$P = 1 - \frac{1}{2(1+x^2)} \qquad (A-7)$$

Appendix B
Integrated precession angle for the electron spin of $^3He^+$ ion in ECR plasma

In this Appendix, we evaluate the integrated precession angle for the electron spin of the $^3He^+$ ion in ECR plasma. For this purpose, our calculation is based on a performance of the 14.5 GHz ECR ionizer developed at Riken assuming that a 500-W microwave power is applied and the ion confinement time is 1 ms.

B-1. Estimation of B_1

The time averaged Poynting vector, i.e. flow of energy density of the electromagnetic wave, for the applied microwave is given by

$$\bar{S} = \bar{u}c, \qquad (B-1)$$

where c is a speed of light, and $\bar{u}$ is the time averaged microwave power per unit volume as given by

$$\bar{u} = \frac{1}{2}\{\epsilon_0 E_1^2 + \mu_0 H_1^2\} \times \frac{1}{2}$$
$$= \frac{1}{2\mu_0} B_1^2, \qquad (B-2)$$

where we use $E_1 = B_1/\sqrt{\epsilon_0\mu_0}$. Substituting Eq. (B-2) for Eq. (B-1), the Poynting vector is expressed by

$$\bar{S} = \frac{cB_1^2}{2\mu_0}. \qquad (B-3)$$

Assuming that that the micro power is P (W), the microwave power penetrating a unit area per second is given by

$$w = \frac{P}{A}, \qquad (B-4)$$

where we take A as the cross section of the wave guide of the microwave for 14.5 GHz, i.e., 2.25 cm^2. From Eq. (B-2) and Eq. (B-4), B_1 is given by

$$B_1 = 60.8\sqrt{P}, \qquad (B-5)$$

where unit of B_1 is mG. If we use P = 500 W, then B_1 is estimated to be 1360 mG.

B-2. Thickness of ESR region: ΔL

We take the direction of mirror field as z, and take the direction normal to the z-axis as r. The thickness of the ESR region ΔL is determined from in homogeneity of the ECR magnetic fields as given by

$$\Delta L \frac{\partial B_q}{\partial q} \approx B_1, \qquad (B-6)$$

where q = z, and r. On the other hand, from the performance of the 14.5 GHz ECR ionizer at Riken, the field gradients are given by

$$\begin{aligned} &\frac{\partial B_z}{\partial z} \sim 380 \quad \text{(Gauss/cm)}, \\ &\frac{\partial B_r}{\partial r} \sim 1900 \quad \text{(Gauss/cm)}, \end{aligned} \qquad (B-7)$$

Substituting Eq. (B-7) for Eq. (B-6), we derive, respectively, thicknesses of the ESR region for the z-direction and r-direction by

$$\Delta L_z \sim 36, \quad (\mu m) \qquad (B-8)$$

$$\Delta L_r \sim 7. \quad (\mu m) \qquad (B-9)$$

Note that the thickness of the ESR region in the z-direction is larger than that in the r-direction as illustrated in Fig. 1 in the text. Assuming that the plasma has a spheroidal shape with a symmetry axis with respect to the z-axis, an averaged thickness is obtained by

$$\Delta L \sim \frac{2\Delta_r + \Delta L_z}{3}$$

$$= 17, \qquad (B-10)$$

which is expressed in unit of μm.

B-3. Effective thickness for ESR region: ΔL^{eff}

It is simply understood that the value presented in Eq. (B-1) is not an actual thickness of the ESR region. We must calculate an effective thickness corrected by the oblique entry or outgoing of the $^3He^+$ ion with respect to direction normal to the plasma wall.

We assume that the plasma wall has a spherical surface with a radius R and an ESR resonance region (a dotted area) with a thickness ΔL as shown in Fig. B-1. Suppose that a $^3He^+$ ion is reflected on the plasma wall with a reflection angle θ relative to the direction normal to the plasma wall. and the reflected/entrance angle of the $^3He^+$ ion distributes isotropically. Here, d is a length of $^3He^+$ ion trajectory which is influenced by an ESR resonance. If θ is smaller than θ_m where the line and the internal circle come in contact with each other, d is approximated by

$$d = \frac{\Delta L}{\cos\theta}, \qquad (B-11)$$

where the terms of d^2, and $(\Delta L)^2$ are neglected. Here, θ_m is given by

$$\theta_m = \sin^{-1}\left\{\frac{R-\Delta R}{R}\right\}. \qquad (B-12)$$

If θ is larger than θ_m, then d is given by

$$d = 2R\cos\theta. \qquad (B-13)$$

Then, d is averaged over θ

$$< d > = \frac{\Delta L \int_0^{2\pi} d\phi \int_0^{\theta_m} \sin\theta d\theta / \cos\theta + \int_0^{2\pi} d\phi \int_{\theta_m}^{\pi/2} 2R\cos\theta\sin\theta d\theta}{\int_0^{2\pi} d\phi \int_0^{\pi/2} \sin\theta d\theta}$$

$$= \Delta L\{-\frac{1}{2} ln(\Delta L/R) + 2\}, \qquad (B-14)$$

where ϕ is an azimuthal angle. An enhancement factor, c_{obl} used in Eq. (7) is, then, given by

$$c_{obl} = -\frac{1}{2} ln(\Delta L/R) + 2$$

$$= 6.0, \qquad (B-15)$$

where R=5 cm and $\Delta L = 1.7 \times 10^{-3}$ cm are used. Then, the effective thickness of the ESR region is given by

$$\begin{aligned} \Delta L^{eff} &= 2c^{obl}\Delta L, \\ &\sim 210, \end{aligned} \qquad (B-16)$$

where Eq. (B-10) and Eq. (B-15) are substituted for Eq. (B-16).

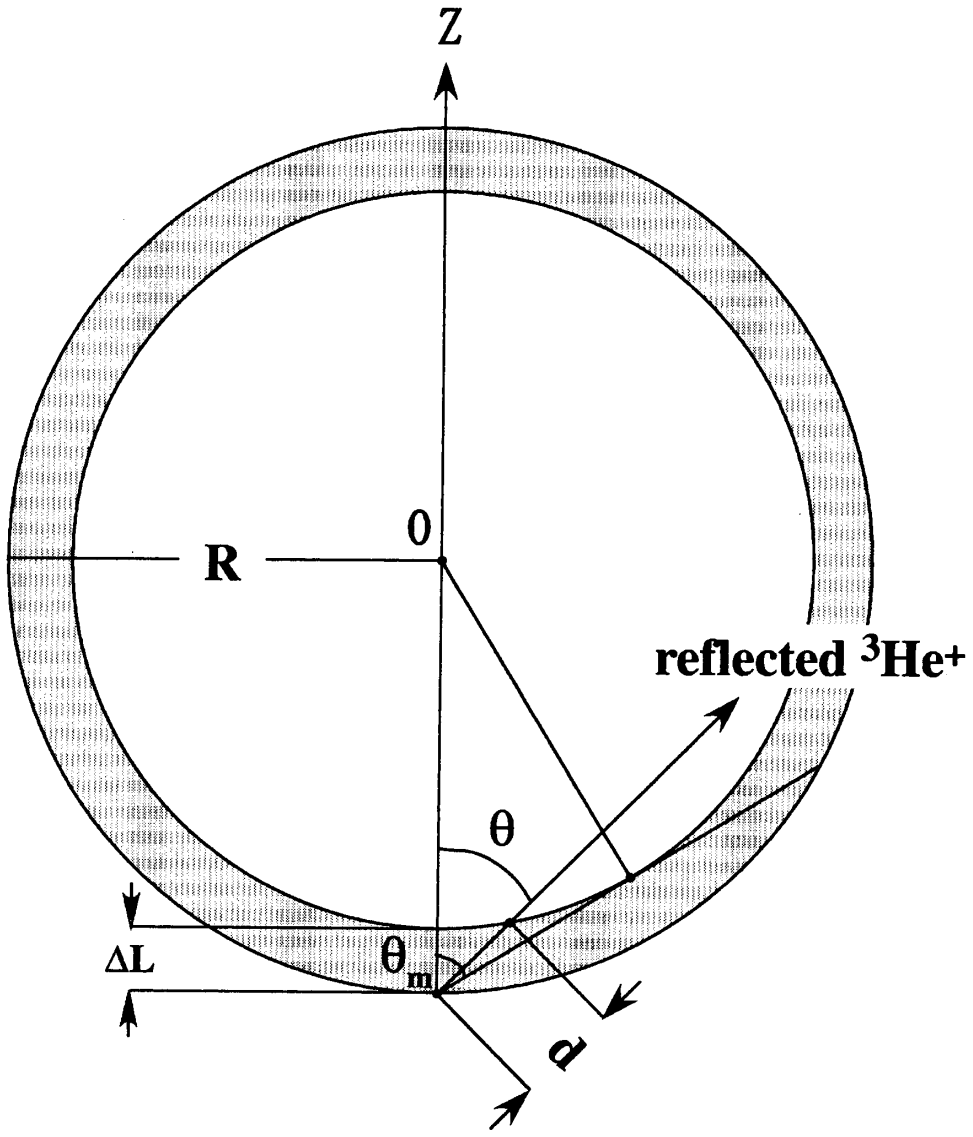

Fig. B-1. Enhancement of ESR region due to oblique entry/exit of $^3He^+$ ion

B-4. Evaluation of precession angle of electron spin

Assuming that the $^3He^+$ ion has a kinetic energy of 5 eV, an effective size of

the plasma is 5 cm, and the ion confinement time is 1 ms, the number of times that the $^3He^+$ ion collides with the plasma wall is obtained by using Eq. (9),

$$N = 357. \qquad (B-17)$$

Consequently, the integrated precession angle of electron spin is obtained by using Eq. (10),

$$\Theta = 2.7 \ \text{(rad.)}. \qquad (B-18)$$